Desalination and Water Treatment
www.deswater.com

doi: 10.5004/dwt.2017.20450

67 (2017) 371–380
March

Developing an effective adsorbent from asphaltene for the efficient removal of dyes in aqueous solution

Mohammad Nahid Siddiqui

Department of Chemistry and Center of Research Excellence in Nanotechnology (CENT), King Fahd University of Petroleum and Minerals, Dhahran 31261, Saudi Arabia, Tel. +966 13 860 2529; email: mnahid@kfupm.edu.sa

Received 17 May 2016; Accepted 16 December 2016

ABSTRACT

A novel adsorbent was prepared by the functionalization of asphaltenes, which were isolated from crude oil and used for the removal of organic pollutants in aqueous solution. The functionalized asphaltenes were characterized by Fourier transform infrared, scanning electron microscope and elemental analysis and found to contain higher amounts of oxygen atoms and carbonyl and hydroxyl functional groups. The impact of different variables such as pH, adsorbent dose, dyes concentration, reaction temperature and contact time were studied during the adsorption process. At 5 h contact time, the best pH for the high efficient adsorption of bromophenol blue (BPB) and methyl orange (MO) were found to be 6.30 and 2.75, respectively. The adsorption isotherms fitted well the Langmuir, Freundlich, Temkin as well as Lagergren models. The adsorption isotherm data of BPB and MO were in good conformity with all models studied, however, BPB was more closely fitted with Freundlich and Temkin isotherms while MO was more closely fitted with Langmuir and Lagergren models thereby implying that the adsorption occurred as a monolayer as well as a heterogeneous surface adsorption. The calculated maximum adsorption capacity for Langmuir model was 7.44 and 2.24 mmol/g for BPB and MO, respectively. Several adsorption kinetic models were fit with experimental data and pseudo-second-order kinetic model was found to be best fitting model. The separation factor (R_L) values found between 0 and 1 that indicates the favorability of the adsorption process on adsorbent surface. The thermodynamic parameters were calculated and the respective values for BPB and MO dyes were found to be $\Delta G°$ (–11.808 and –14.057 kJ/mol), $\Delta H°$ (8.509 and 6.460 kJ/mol) and $\Delta S°$ (65.954 and 66.613 J/K mol), which exhibited that the adsorption of dyes on functionalized asphaltenes was spontaneous, endothermic with increased randomness. The functionalized asphaltene showed high adsorption capacity with highly efficient removal for BPB and MO dyes.

Keywords: Functionalized asphaltenes; Adsorption; Dyes; Water pollutants; Novel adsorbent

1. Introduction

Crude oil consumption has raised drastically as fuel and energy source in comparison to other alternate energy resources. About 70% from the heavy crude oil residue is drilled oil and very small amount is being used without significant process [1]. One of the fractions considered as a most troublemaker in the refinery and cracking processing of the petroleum is asphaltenes due to the precipitation behaviour of the asphaltenes, which can reduce the flow of the oil and can lead to blockage problems in several equipments [2]. In addition, asphaltenes can form sludge and can poison or deactivate the hydrodesulfurization and hydrocracking catalysts, which leads to the reduction of conversion efficiency for the two processes [3,4]. The structure of these compounds was very difficult to study due to their chemical complicity composition, it was reported that this material is composed of polyaromatic groups in the centre connected

with alicyclic and aliphatic groups with some heteroatoms and metals [5,6].

The dyes are complex organic compounds that have ability to be attached with the surface and impart the color [7]. These dye contaminants have negative impact on the environment that is why the removal and degradation of these compounds took a significant attraction. Dyes such as bromophenol blue (BPB) and methyl orange (MO), widely used in textile and tannery may have some health hazards. These dyes may cause eye and skin irritation, respiratory and digestive tract irritation, gastrointestinal irritation with nausea, vomiting and diarrhoea, anaemia, insomnia, renal damages, central nervous system damage and dysfunction of the immune system [8–10]. A number of methods have been developed and reported for the removal of dyes such as precipitation, ion exchange, reverse osmosis and adsorption, of these; adsorption has proved itself as one of the best methods [11–17].

Different sorbents were investigated for the removal of the dyes from the wastewater, one of these sorbents is the activated carbon which is a very famous sorbent for the removal of dyes from wastewater [18], due to its high adsorption efficiency comparing with many different sorbents, however, the activated carbon has some drawbacks such as the relative high cost, non-selectivity and regeneration problems [19]. Agricultural wastes have also been used for the removal of the dyes for the aqueous media, which contain some organic compounds that can remove the dyes [20]. In addition, industrial solid waste such as sludge of metal hydroxide was reported to have high removal efficiency for azo dyes in aqueous sample [21], these wastes are very cost effective, available and have high adsorption capacity, and however, these wastes may contain some hazardous materials such as heavy metals [22].

Carbon nanotubes and their corresponding composites have been widely investigated and revealed an excellent adsorption capacity due to the high surface area of these materials [23], but the drawbacks of these nanomaterials are the high cost and the difficulty of collection after adsorption, due to the highly dispersion because of the size make the industrial applications very challenging [24].

In this work, the asphaltenes were isolated and functionalized as adsorbent for the removal of organic water pollutants such as dyes. Dyes may interact with functionalized asphaltenes through hydrophobic interactions. π–π bonding generally takes place between bulk π system of functionalized asphaltenes and dye molecules with C=C or benzene rings [25]. The functional groups such as –COOH, –OH and $–NH_2$ are responsible for the hydrogen bonding between the functionalized asphaltenes and the contaminant [26]. Due to the charged surface of functionalized asphaltenes, the adsorption is also controlled by electrostatic interaction [27]. Therefore, the novelty of this work is to make best use of the undesired fraction of crude oil, asphaltenes and to convert it to effective adsorbent by functionalization for the efficient removal of dyes from the aqueous medium. Use of asphaltenes or functionalized asphaltenes as adsorbents has not been reported in the literature yet. Therefore, in this study, we focussed to develop a novel adsorbent as functionalized asphaltenes for the efficient removal of dyes in aqueous solution.

2. Experimental setup

2.1. Asphaltenes separation

7.0 g of Arabian heavy residue was transferred to a beaker and heated with a very small amount of *n*-heptane. The solution was mixed properly and transferred to 2 L container, and then to this solution 700 mL of *n*-heptane was added. The solution was placed in a mechanical shaker with a water bath. In order to increase the residue solubility in the heptane it was heated at 90°C for 2 h with continuous stirring. Then, the solution was covered using aluminum foil and was stand for cooling for overnight. The gradual cooling helps to produce efficient precipitation of asphaltenes. After that, the solution was filtered with 0.8 μm pore size filter paper. The residue was extracted by Soxhlet using toluene as extracting solvent, and the extract was filtered with the same microfilter paper. After the evaporation of extract, the asphaltenes were collected in beaker. Then, it was washed several times with small amount of *n*-heptane. Finally, the solid asphaltene was dried at 105°C for 2 h.

2.2. Functionalization of asphaltenes

10 g of the asphaltenes were dispersed in 200 mL nitric acid (70%) and the mixture was sonicated for 60 min. The sonicated mixture was refluxed for 45 min at 80°C and then cooled to room temperature and left overnight. The treated asphaltenes mixture was filtered using Whatman No. 1 filter paper and washed with deionized water several times until the washings became clear with pH adjusts in the range of 6–7. Next, the treated asphaltenes were dried for 24 h in an oven at 80°C and pulverized in a ball mill. The treated asphaltenes were characterized by several analytical techniques.

2.3. Dyes and solvents

BPB, MO and solvents were procured from British Drug Houses (BDH), London, UK. The chemical structures of both dyes are as follows. The reagents used were of AR grade.

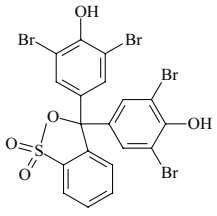

Bromophenol blue

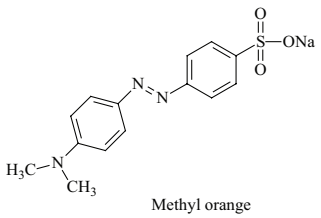

Methyl orange

Properties	Methyl orange	Bromophenol blue
Chemical formula	$C_{14}H_{14}N_3NaO_3S$	$C_{19}H_9Br_4NaO_5S$
Molecular weight (g/mol)	327.334	691.94
Density (g/cm^3)	0.97	2.2

2.4. Sample characterization

The functionalized asphaltenes were characterized using scanning electron microscope (SEM), Fourier transform infrared (FTIR) and elemental analysis techniques.

2.5. Adsorption experiments

The adsorption properties of the adsorbent for BPB and MO were determined by spectrophotometric method; the procedure followed for adsorption of dyes involves: a mixture of adsorbent (200 mg) in 25 mL of 25 mg/L dye solution was stirred using a temperature-controlled shaker bath at various pH for overnight. The adsorbent was filtered and the filtrate was then analyzed by UV–Vis spectrophotometer to find out the remaining dye concentration.

The capacity of adsorption (q_{dye}) was calculated by Eq. (1):

$$q_{dye} = \frac{(C_i - C_e)V}{W} \text{ mmol / g} \quad (1)$$

where C_i and C_e are the initial and equilibrium concentrations of dye, respectively, W is the weight of the adsorbent in g and V is the volume of the solution in mL.

Adsorption kinetic studies were carried out by stirring 25 mL of 25 mg/L (ppm) dye solution in a preferred pH buffer with adsorbent (200 mg) at different temperatures and to determine the dye concentrations by taking a small amount of filtered aliquots at various time intervals. Adsorption isotherms were constructed by determining the adsorption capacities of the adsorbent at different dye concentration ranging from 10 to 100 mg/L (ppm) at ambient temperature. By carrying out experiments at different temperatures, thermodynamic parameters such as change in enthalpy $\Delta H°$, change in free energy $\Delta G°$ and change in entropy $\Delta S°$ were calculated.

3. Results and discussion

3.1. Characterization of functionalized asphaltenes by FTIR, SEM and elemental analysis

The functionalized asphaltenes were characterized by using different analytical techniques such as FTIR, SEM and elemental analysis.

FTIR spectra of asphaltenes and functionalized asphaltenes were recorded as shown in Fig. 1. The most visible and significant difference in these two IR spectra is the appearance of peaks around carbonyl, hydroxyl and amino regions in functionalized asphaltenes. The IR spectra of functionalized asphaltene show the presence of strong peaks of several important functional groups such as C=O at 1,721 cm^{-1}, carboxylate ion at 1,533 cm^{-1} and low intensity peak at 1,342 cm^{-1} representing C–O group. The appearance of these peaks in functionalized asphaltene confirms the formation of carbonyl and carboxylic groups on the surface of asphaltenes on functionalization treatment. The hydroxyl groups are enveloped in big hump between 3,300 and 3,700 cm^{-1} [28–30]. A significantly strong peak observed for amide group with C=O stretching vibrations at 1,627 cm^{-1} and N–H stretching vibration of amide group at 3,454 cm^{-1}. The appearance and identification of these C=O peaks from carboxylic and amide groups confirms the functionalization of asphaltenes.

SEM images for asphaltenes and functionalized asphaltenes are shown in Figs. 2 and 3 for the morphological studies. It can be observed clearly from the images that there are differences in the surface, shape and the morphology those were redecorated from soft surface in the asphaltene to more rough and magnified shape in functionalized asphaltenes. Both asphaltenes are magnified in the same scale to assess the real-time morphological changes occurred in asphaltene on functionalization. The changes are ascribed to the introduction of the different functional groups on the surface of asphaltenes on the functionalization process.

The elemental analysis of asphaltenes and functionalized asphaltenes is given in Table 1. The virgin asphaltenes contain significantly higher amount of carbon and lower amount of hydrogen atoms. This is due to the presence of highly condensed aromatic ring structures and some aliphatic chains. Other elements such as N and O are present in lower amounts while S is present in significant amount as the part

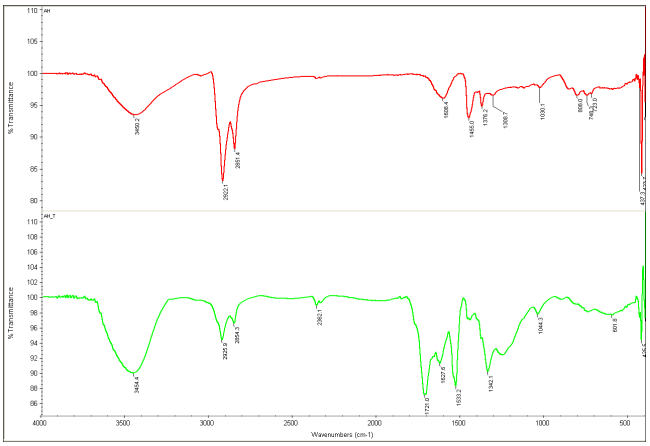

Fig. 1. FTIR spectra of Arab heavy (AH) virgin asphaltenes and below functionalized asphaltenes.

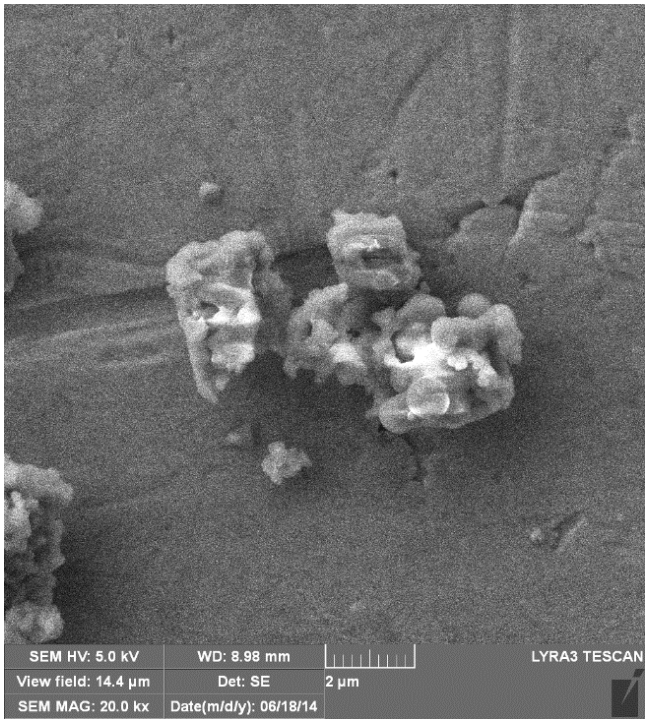

Fig. 2. SEM of AH virgin asphaltenes.

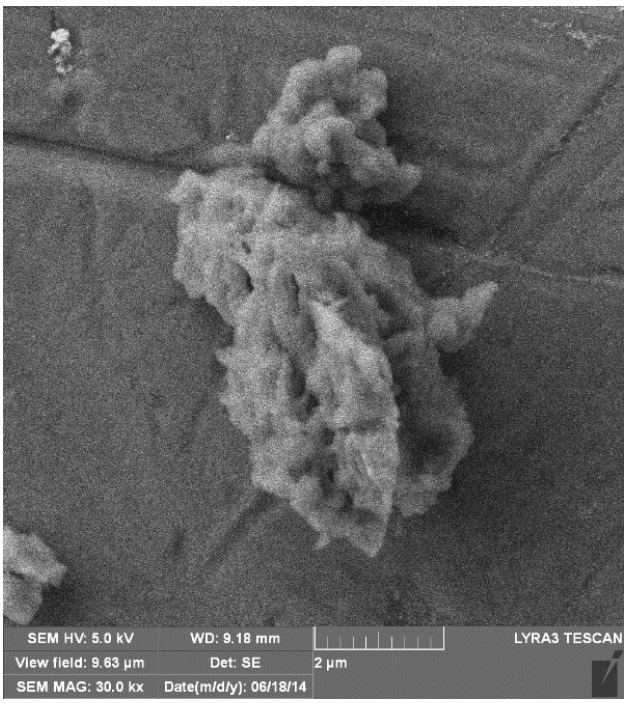

Fig. 3. SEM of AH functionalized asphaltenes.

Table 1
Elemental analysis in percentage (%)

Sample	C	H	N	S	O (by difference)
AH	81.28	7.44	1.19	7.17	2.92
AH-F	57.08	4.13	5.31	5.65	27.83

Note: AH – Arab heavy.

of aromatic ring structures. The elemental composition of the asphaltenes changed drastically after functionalization. The carbon contents decreased from 81.28% to 57.08% and hydrogen contents decreased from 7.44% to 4.13%. There are also changes in the contents of N and S atoms, however, the most significant change observed in the contents of oxygen atoms. The oxygen contents increased from merely 2.92% to 27.83%. The increase in oxygen contents in the functionalized asphaltenes is attributed mainly to the formation of carbonyl, ether, carboxylic and lactam groups at the cost of peripheral carbon chains. A significant numbers of peripheral carbon chains are assumed to be lost by converting into CO_2, CO and other hydrocarbon gases on acid treatments thus leading to the loss of carbon contents and increase of oxygen contents. This transformation is chiefly responsible for the increased adsorptive behaviour of functionalized asphaltenes [28–30].

3.2. Effect of pH

pH of the solution plays important role in determining the efficiency of a sorption process. The surface properties of the adsorbents and the degree of ionization vary with the variation of the pH of the solution. The experiments were carried out at a range of pH between 2.5 and 11.0 using

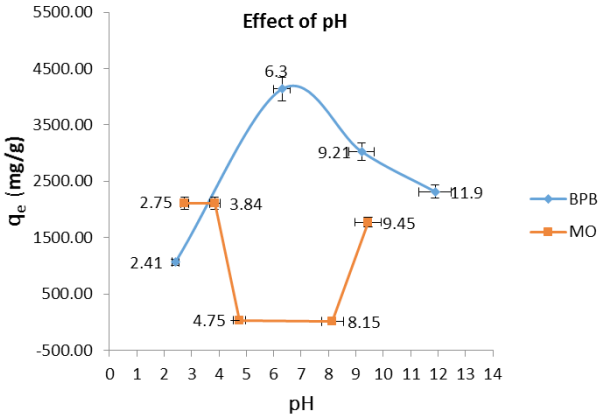

Fig. 4. pH dependence of dyes uptake by adsorbent.

acetate buffer, to find out its effect on uptake of BPB and MO dye by adsorbent. pH has a very strong effect on the adsorption capacities of the adsorbent as can be seen in Fig. 4. The optimum pH was found to be 6.30 for BPB and 2.75 for MO. The adsorption of MO slightly decreased from pH 2.75 to 3.84 and then sharply decreased at 4.57–8.15 before increasing at pH 9.45. This phenomenon is ascribed to the protonation of the functional groups available on the surface of functionalized asphaltenes when H^+ is responsible for facilitating in providing strong interaction between the surface of the adsorbent and dye leading to the more adsorption of the dye [15,17]. At lower pH, more H^+ are available which facilitate stronger electrostatic interaction between positively charged amino groups present on the surface of adsorbent and negatively charged dye anions. Similarly, the decrease in adsorption at higher pH can be attributed to the changes occurred at the surface of the adsorbents such as the protonation of amino groups and chemical bonding of MO with the functional groups of the dye. With the increase of pH, the positive charge of the surface of the adsorbents decreased significantly and the number of negative charged sites increased leading to the lower interaction between absorbent and dye. The adsorption of MO at pH 7 is almost negligible or zero while it is 2.20 mg/g at pH 2.7 that drop in the adsorption capacity is attributed to the changes in the charge of MO at pH more than 7 [31]. This shows very beneficial property of the adsorbent that optimum adsorption of the MO can to be achieved between pH 2 and 3 while desorption will be effective between pH 6 and 7. Hence, charging and discharging of dye is pH controlled. With the increase of pH, the number of OH^- sites increases in the adsorbents significantly, which lead to the repulsion with negatively charged dye thus affording low adsorption. However, BPB shows the maximum adsorption at pH 6.30 on the same adsorbent which is attributed to its chemical structure and properties. A hypothetical adsorption process of MO and BPB on functionalized asphaltene is shown in Fig. 5.

3.3. Effect of contact time

A plot of adsorption capacity vs. time determines adsorption rate in Fig. 6. The graph shows the adsorption takes place

in two distinct steps. In first step, the adsorption started very fast from the first 5 to 60 min. This pattern shows the high degree of adsorbing affinities of the adsorbent for MO and BPB dyes. This phenomenon can be explained as the maximum availability of the activated sites on the surface of the adsorbents [15,17]. In the second step, the adsorption rate further increased until 120 min then slowed down to attain the equilibrium. This slow down process can be attributed to the non-availability of the bonding sites on adsorbents, steric hindrance or crowding of absorbed material on the surface and repulsion between adsorbed dyes and incoming dyes molecules. It was found in our study that the adsorption equilibrium reached in about 5 h where lines became plateau indicating the saturation points and non-availability of any more free sites.

3.4. Effect of amount of adsorbent

In order to calculate the optimized amount of absorbent, different amounts of the adsorbent were reacted with the constant initial concentration of 25 ppm of MO and BPB dye solutions for 120 min. The availability of reactive sites on adsorbent is an important parameter, which determines the number of free adsorption sites available for the adsorption processes. Fig. 7 shows that the degree of dyes adsorption increased with the increase of adsorbent mass. This increase in the percentage of adsorption of the dyes is attributed to the availability of the large number reactive sites on the adsorbent, which were increasing with the quantity of adsorbent.

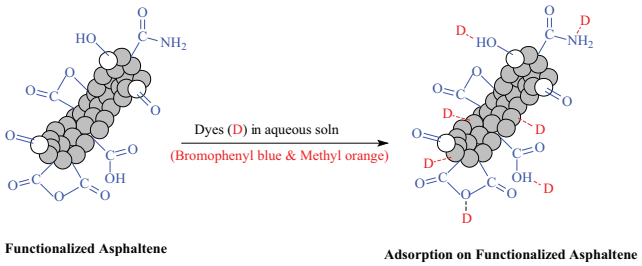

Fig. 5. Hypothetical adsorption of MO and BPB dyes on functionalized asphaltenes.

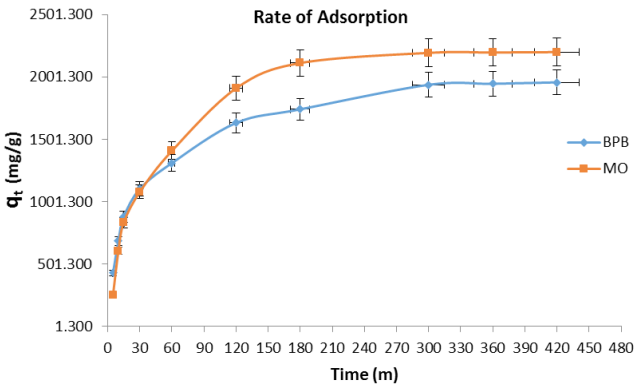

Fig. 6. Adsorption curves with the time of 25 ppm for MO and BPB solution at their optimum pH.

Initially, the adsorption of the amount of dyes increased rapidly with increase of the amount of adsorbent; however, after equilibrium, the amount of dyes adsorption started decreasing. This higher uptake of dyes can be attributed to an increase in free adsorption sites on the surface of adsorbent. However, the decrease in the adsorption of dyes with increased amount of adsorption is attributed to the limited volume of solution starts an agglomeration of the adsorbent leading to the reduction of the intercellular distances. The maximum adsorption for MO and BPB dyes was achieved at 0.4 g of adsorbent mass. This increase in dose amount leads to prevent the access to adsorption site that literally means overlapping of adsorption sites due to the overcrowding or steric hindrance created by the adsorbed dye molecules.

3.5. Effect of initial concentration

The adsorption capacity of adsorbent increases with increasing concentrations of MO and BPB dyes is shown in Fig. 8. The effect of MO and BPD dyes concentration was studied in the range of 5, 10, 25, 50, 75 and 100 ppm concentrations while other parameters kept constant. The adsorption

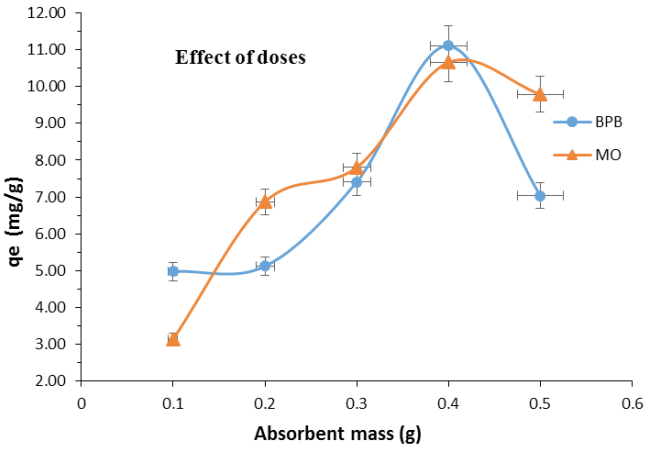

Fig. 7. The effect of amount of adsorbent on the adsorption of MO and BPB dyes.

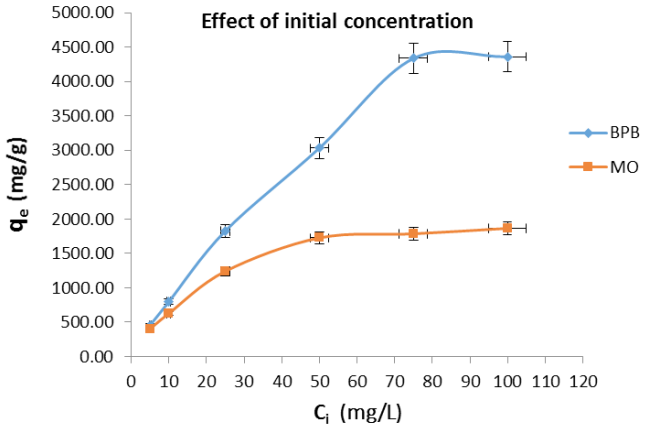

Fig. 8. The initial concentration effect on the adsorption of dyes at pH 6.3 for BPB and pH 2.7 for MO 5 h at 295 K.

capacity was rapidly increased up to the equilibrium (50 ppm) for MO and 75 ppm for BPB. A higher initial dye concentration is instrumental for the increase of adsorption, which acts as a driving force for the attraction of dye molecules from solution to the surface of functionalized asphaltene. After attaining the adsorption equilibrium, the adsorption capacity of the absorbent was slowed down affording a plateau. This tendency can be attributed to the saturation of the active free sites on the surface of adsorbent that led to no additional adsorption of the dye molecules.

3.6. Effect of temperature

Fig. 9 shows the effect of the temperature on adsorption of dyes. Temperature is one of the most important parameter used for the study adsorption processes. Our adsorption studies were carried out with initial dye concentrations in batch processes at three different temperatures more specifically at 308, 318 and 328 K. Fig. 7 indicates that with the increase of temperature, the adsorption of dyes increased steadily. This phenomenon can be explained as the higher temperatures may be forcing strong mobilization of dye molecules leading to the lowering of the activation energy resulting more adsorption on the functional groups available on the surface of the adsorbent and enhancing the rate of intraparticle diffusion. Furthermore, high temperature leads to the more solubility of the dye in the solution leading to more adsorption. Hence, the adsorption efficiency increases with increasing temperature that shows the adsorption process is endothermic.

3.7. Adsorption isotherms

The thermodynamic parameters were obtained from the adsorption experiment, and the results were explained in Fig. 7. Lagergren adsorption kinetic model has been reported as an optimum method to study the adsorption properties. The kinetic orders were expressed by Eqs. (2) and (3) (first- and second-order models, respectively)

$$\log(q_e - q_t) = \log q_e - \frac{k_1 t}{2.303} \tag{2}$$

$$\frac{t}{q_t} = \frac{1}{k_2 q_e^2} + \frac{t}{q_e} \tag{3}$$

where k_1 is first-order constant and k_2 is the second-order rate constant; q_t and q_e are the capacities of the adsorption for the adsorbent at time t and at respective l. Although BPB and MO both gave regression value (R^2) above 0.99 for the pseudo-first-order Lagergren kinetic model, but there is a vast difference between the values of experimental adsorption capacity and the calculated adsorption capacity. Therefore, the graph that shows the kinetic model hasn't been displayed, while the MO and BPB were fitted the second-order model as shown in Fig. 10 with very close experimental adsorption capacity and the calculated adsorption capacity given in Table 2.

The values represented in Table 2 showed that rate constant for the BPB removal is greater than MO constant; however, adsorbent adsorbed greater amount of MO with the time as shown in Fig. 10. The adsorption capacity of MO is found to be

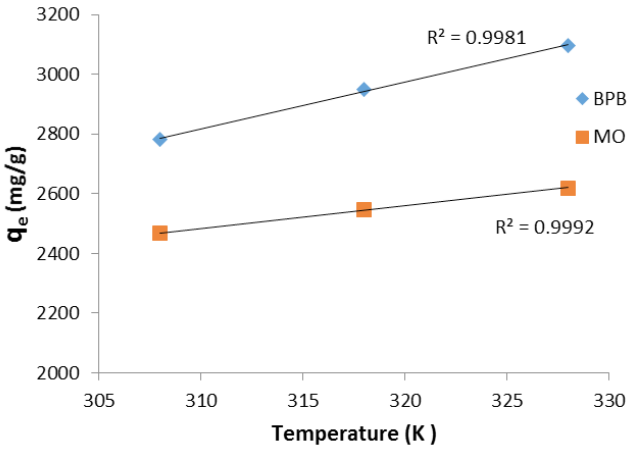

Fig. 9. Effect of temperature on the adsorption capacity of adsorbent.

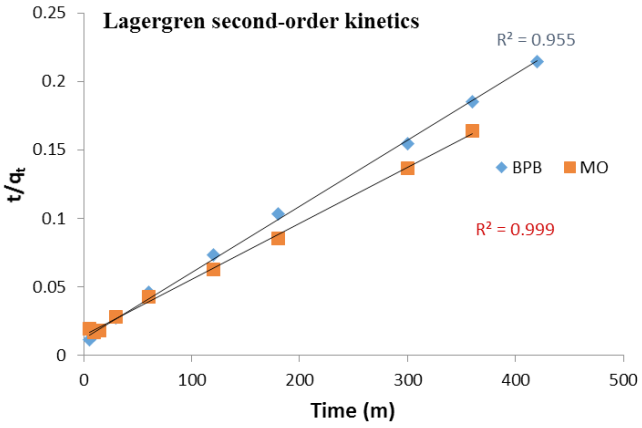

Fig. 10. Adsorption pseudo-second-order model for MO and BPB at 295 K.

Table 2
Lagergren pseudo-second-order kinetic model parameters for MO and BPB adsorption

Lagergren second-order kinetic	$q_{e\,(Calc)}$ (mg/g)	K_2 (h g/mg)	$q_{e\,(Exp)}$ (mg/g)	h^a (h g/mg)	R^2
BPB/295 K	2.33	0.35	1.96	1.89	0.955
MO/295 K	2.37	1.00	2.20	5.62	0.999

[a]Initial adsorption rate $h = k_2 q_e^2$.

Table 3
Langmuir isotherm model constants for MO and BPB removal

Langmuir isotherm model				
Entry No.	Dye	Q_m (mmol/g)	b (dm³/mmol)	R^2
1	BPB	7.44	0.031	0.950
2	MO	2.236	0.069	0.990

a little higher than that of BPB. This significant difference can be explained due to the lower effective ionic radii of BPB than that of MO and affinity differences of motifs of phosphonate in the adsorbent for the dye [31]. The results showed that the functionalized asphaltenes is an excellent adsorbent for the adsorption of MO and BPB dyes in aqueous solutions.

The Langmuir isotherm is based on the assumptions that on structurally homogeneous adsorbent, all adsorption sites are energetically equivalent and identical as well as the intermolecular force decreases rapidly with distance.

It follows the mechanism as adsorption of monolayer on the adsorbent surface. The Langmuir constants and adsorption capacities can easily be calculated by linearized Langmuir isotherm (Eq. (4)) as follows:

$$\frac{C_e}{q_e} = \frac{C_e}{Q_m} - \frac{1}{Q_m b} \tag{4}$$

where q_e is mmol of dye adsorbed per gram of the adsorbent; C_e is dye residual concentration in solution at equilibrium, Q_m is the maximum specific uptake (maximum adsorption capacity) corresponding to the site saturation and b is the ratio of adsorption and desorption rates, the Langmuir constant [32]. Table 3 showed the maximum adsorption capacity and ratio of adsorption and desorption rates obtained by Langmuir model. Fig. 11 represents the plot of C_e/q_e vs. C_e.

In general, Langmuir model assumes that fixed number of adsorption sites is available, uniformly distributed on the surface of adsorbent, exhibiting monolayer, and releases certain amount of heat during the adsorption process taken place on adsorbent surface. At large, the surface coverage will be reduced by increasing the surface temperature of the adsorbent. Here one of the key assumptions of the Langmuir isotherm is simplified to fit in the study that the adsorption takes place only at specific localized sites on the surface and the saturation coverage corresponds to complete occupancy of these sites. This assumption is applicable in this study also.

The affinity of the adsorption of the dyes on the adsorbent surface can be described by the separation factor (R_L) in Langmuir isotherm from Fig. 11 [33]:

$$R_L = \frac{1}{(1+bC_0)} \tag{5}$$

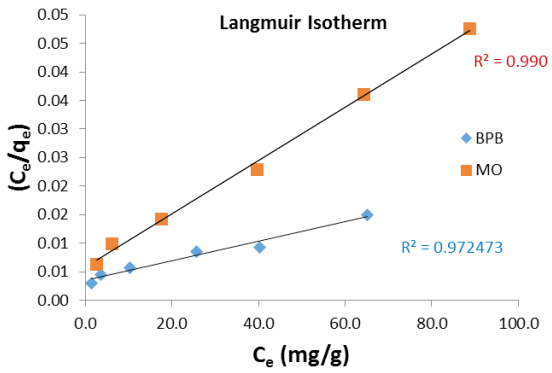

Fig. 11. Adsorption Langmuir isotherm of MO and BPB on adsorbent.

where C_0 is the initial dye concentration and b is the Langmuir equilibrium constant. When the value of R_L falls between 0 and 1, it indicates the favorability of the adsorption on adsorbent surface. Table 4 clearly show that the R_L values falls in the range mentioned, and that means good adsorption favorability for the dyes on the functionalized asphaltene surface.

A list of different adsorbent with their maximum adsorption capacities (q_{max}) values obtained by Langmuir isotherm of MO is provided in Table 5.

On the other hand, Freundlich isotherm model describes the non-ideal adsorption occurring on a heterogeneous surface with uniform energy as well as multilayer adsorption; as the model was expressed by Eqs. (6) and (7):

$$q_e = k_f C_e^{1/n} \tag{6}$$

$$\log q_e = \log k_f + \frac{1}{n}\log C_e \tag{7}$$

where q_e the concentration at the equilibrium of the dyes on the adsorbent and C_e on the sample solution; k_f and n are

Table 4
The R_L values based on the Langmuir isotherm model

C_i (mg dm^{-3})	R_L value	
	BPB	MO
10	0.7621	0.5913
25	0.5617	0.3666
50	0.3905	0.2244
75	0.2993	0.1617
100	0.2426	0.1264

Table 5
A comparative analysis of Q_m values of Langmuir adsorption using various adsorbents for MO

No.	Adsorbents	Q_m (mg/g)	References
1	Egussi peeling	13.889	[15]
2	Rice husk	1.295	[15]
3	Lapindo volcanic mud	333.33	[17]
4	Pine cone derived activated carbon	404.4	[34]
5	Banana peel	21	[35]
6	Orange peel	20.5	[35]
7	Calcined layered double hydroxides	200	[36]
8	Zn/Al-layered double hydroxides	181.9	[36]
9	Hypercrosslinked polymeric absorbents	70.9	[37]
10	Diaminoethane sporopollenin biopolymer	4.7	[38]
11	Activated alumina	9.8	[39]
12	Bottom ash	3.6	[40]
13	Functionalized asphaltenes (mmol/g)	2.24	This study

Table 6
Freundlich isotherm model constants for MO and BPB removal

Freundlich isotherm model					
Entry No.	Dye	N	$1/n$	k_f	R^2
1	BPB	1.458	0.686	0.342	0.995
2	MO	2.165	0.462	0.293	0.943

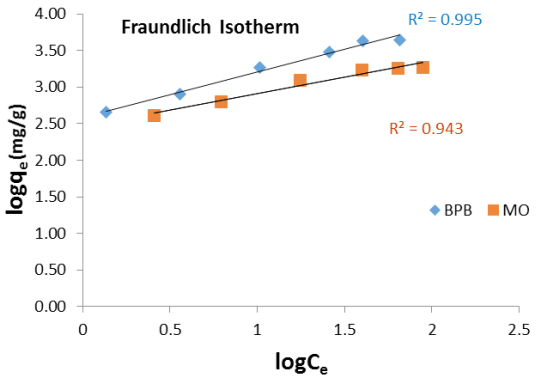

Fig. 12. Adsorption Freundlich isotherm of MO and BPB on adsorbent.

Freundlich constants, given in Table 6, can be calculated from the slope and intercept of the linear plot of $\log q_e$ vs. $\log C_e$ as given in Fig. 12. The values of n were found to be higher than one and the model explains if values of n are in the range of 1–10 then that should be considered as favorable adsorption classification. The range of 0–1 for slope ($1/n$) is considered a measure of surface heterogeneity or adsorption intensity, indicating more heterogeneous nature as its $1/n$ value gets closer to zero. A $1/n$ value below unity is indicative of chemisorption process, whereas $1/n$ above one implies cooperative adsorption (Table 6). For the adsorption of BPB dye, the higher values of the constant k_f(0.342), which is related to adsorption capacity (q), indicates higher affinity of the dye to the adsorbent in comparison to MO adsorption that has relatively lower values of the constant k_f(0.293).

The Temkin thermodynamic adsorption model is experimentally and theoretically forthright and applicable to the sets of isothermal data. The Temkin adsorption model provides significant thermodynamic values such as enthalpy and entropy of adsorption, which proved to be very useful characterizing and explaining the differences between various surfaces.

The Temkin isotherm equation suggests that owing to adsorbent–adsorbate interactions, the heat of adsorption of molecules in layer decreases linearly with increasing coverage, and the adsorption is characterized by a uniform distribution of the bond energies [41]. The Temkin isotherm model is an extension of the Langmuir thermodynamic model that integrates a linear variation of the enthalpy of adsorption. The Temkin thermodynamic model can be interpreted in two distinctive physical states: the first assumption is based on adsorbent–adsorbate interactions where the equivalent binding surface and an adsorption enthalpy varies with coverage, while the second assumption is based on the heterogeneity of surface which lead to the variations in the uniform distribution of heterogeneous binding surfaces and an adsorption enthalpy.

The Temkin isotherm can be expressed by the following equation:

$$q_e = \frac{RT}{b}\ln(AC_e) \tag{8}$$

Moreover, Eq. (8) can be linearized as:

$$q_e = B\ln A + B\ln C_e \tag{9}$$

where B corresponds to the adsorption potential of the adsorbent (kJ/mol), A is the Temkin isotherm constant (L/g). A plot of q_e vs. lnC_e, in Fig. 13, is used to calculate the Temkin isotherm constants A and B and values are tabulated in Table 7.

It can be inferred from Figs. 11–13, that the adsorption of the MO and BPB dyes on the surface of functionalized asphaltenes could be heterogeneous or monolayer because the adsorptions obeyed all three Langmuir, Freundlich and Temkin isotherms.

3.8. Thermodynamic analyses of the adsorption isotherm data

The thermodynamic parameters were calculated using Fig. 14 and Eq. (10) and are tabulated in Table 8 [42,43].

The negative free energies $\Delta G°$ confirms the spontaneity of the process.

$$\log\left(\frac{q_e}{C_e}\right) = -\frac{\Delta H}{2.303RT} + \frac{\Delta S}{2.303R} \tag{10}$$

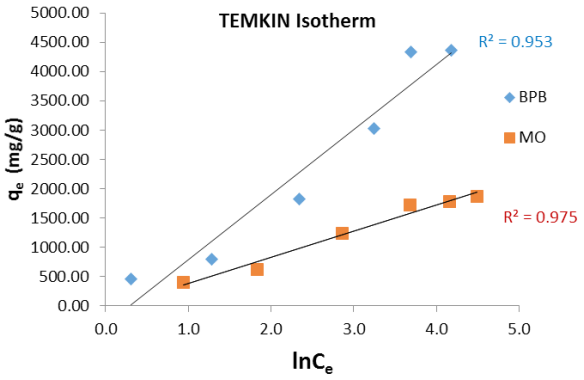

Fig. 13. Adsorption Temkin isotherm of MO and BPB on adsorbent.

Table 7
Temkin isotherm model constants for MO and BPB removal

Temkin isotherm model				
Entry No.	Dye	B	A	R^2
1	BPB	1.3981	0.425	0.953
2	MO	0.5199	0.579	0.975

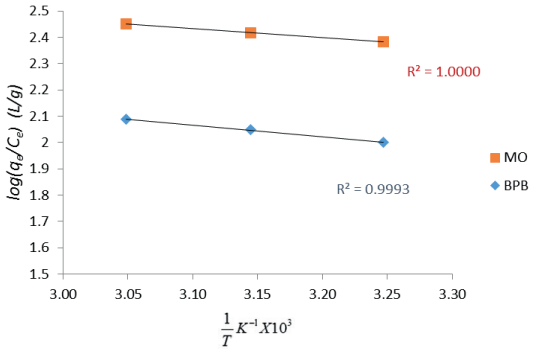

Fig. 14. Plot of $\log(q_e/C_e)$ vs. $1/T$ (K) for the calculation of thermodynamic parameters.

Table 8
Thermodynamic data for BPB and MO adsorption

Dye	Temp (K)	$\Delta G°$ (kJ/mol)	$\Delta H°$ (kJ/mol)	$\Delta S°$ (J/K mol)	R^2
BPB	308	–11.805	8.509	65.954	0.9993
MO	308	–14.057	6.460	66.613	1.000

The negativity of $\Delta G°$ increases with the temperature, which shows that the adsorption is more favorable at higher temperatures. Favorable adsorption at higher temperatures is attributed to the greater swelling of the adsorbent and increased diffusion of dyes into the adsorbent. The positive enthalpies $\Delta H°$ confirm that the adsorption process is endothermic. In addition, it can be found in Table 8 that the $\Delta S°$ values are positive, suggesting that the randomness increased during adsorption of dye because of release of water molecules from the large hydration shells of the dye.

4. Conclusion

A novel adsorbent was prepared by the functionalization of asphaltenes, which were isolated from crude oil and highly undesirable and problematic part of the petroleum matrix. Asphaltenes were functionalized using acid and used for the removal of organic pollutants in aqueous solution. The impact of different variables such as pH, adsorbent dose, dyes concentration, reaction temperature and contact time were studied during the adsorption process. At 5 h contact time, the best pH for the high efficient adsorption of BPB and MO were found. The adsorption isotherms fitted well the Langmuir, Freundlich, Temkin as well as Lagergren models. The adsorption isotherm data of BPB and MO were in good conformity with all models studied; however, BPB was more closely fitted with Freundlich and Temkin isotherm while MO was more closely fitted with Langmuir and Lagergren models thereby implying that the adsorption occurred as a monolayer as well as a heterogeneous surface adsorption. The calculated maximum adsorption capacity for Langmuir model was good. Several adsorption kinetic models were fit with experimental data and pseudo-second-order kinetic model was found to be best fitting model. The separation factor (R_L) values indicated the favorability of the adsorption process on adsorbent surface. The thermodynamic parameters were calculated for BPB and MO dyes that exhibited that the adsorption of dyes on functionalized asphaltenes was spontaneous, endothermic with increased randomness. The functionalized asphaltene showed high adsorption capacity with highly efficient removal for BPB and MO dyes.

Acknowledgments

The author would like to acknowledge the support provided by the Deanship of Scientific Research (DSR) at King Fahd University of Petroleum and Minerals (KFUPM), Dhahran, Saudi Arabia, for funding this work through project number SB141007.

References

[1] J.G. Speight, Fuel Science and Technology Handbook, Marcel Dekkar, New York, 1990.
[2] M. Mousavi, T. Abdollahi, F. Pahlavan, E.H. Fini, The influence of asphaltene-resin molecular interactions on the colloidal stability of crude oil, Fuel, 183 (2016) 262–271.
[3] C.H. Bartholomew, Upgrading of Heavy Oils and Residue, M.C. Oballa, S.S. Shih, Eds., Catalytic Hydroprocessing of Petroleum and Distillates, Marcel Decker, New York, 1994, p. 42.
[4] P. Painter, B. Veytsman, J. Youtcheff, Asphaltene aggregation and solubility, Energy Fuels, 29 (2015) 2120–2133.
[5] M. Hasan, M.N. Siddiqui, M. Arab, Separation and characterization of asphaltenes from Saudi Arabian crudes, Fuel, 67 (1988) 1131–1134.
[6] J.W. Shirokoff, M.N. Siddiqui, M.F. Ali, Characterization of the structure of Saudi crude asphaltenes by X-ray diffraction, Energy Fuels, 11 (1997) 561–565.
[7] J. Sokolowska-Gajda, H.S. Freeman, A. Reife, Synthetic dyes based on environmental considerations, Dye Pigm., 30 (1996) 1–20.
[8] G. Camci-Unal, N.L.B. Pohl, Quantitative determination of heavy metal contaminant complexation by the carbohydrate polymer chitin, J. Chem. Eng. Data, 55 (2010) 1117–1121.
[9] R. Kiefer, W.H. Höll, Sorption of heavy metals onto selective ion-exchange adsorbents with aminophosphonate functional groups, Ind. Eng. Chem. Res., 40 (2001) 4570–4576.
[10] G. Güçlü, G. Gürdağ, S. Özgümüş, Competitive removal of heavy metal ions by cellulose graft copolymers, J. Appl. Polym. Sci., 90 (2003) 2034–2039.
[11] M.V. Subbaiah, D.S. Kim, Adsorption of methyl orange from aqueous solution by aminated pumpkin seed powder: kinetics, isotherms, and thermodynamic studies, Ecotoxicol. Environ. Saf., 128 (2016) 109–117.
[12] L. Ai, C. Zhang, L. Meng, Adsorption of methyl orange from aqueous solution on hydrothermal synthesized Mg–Al layered double hydroxide, J. Chem. Eng. Data, 56 (2011) 4217–4225.
[13] E. Mekatel, S. Amokrane, A. Aid, D. Nibou, M. Trari, Adsorption of methyl orange on nanoparticles of a synthetic zeolite NaA/CuO, C.R. Chim., 18 (2015) 336–344.
[14] K. Mahmoudi, N. Hamdi, A. Kriaa, E. Srasra, Adsorption of methyl orange using activated carbon prepared from lignin by $ZnCl_2$ treatment, Russ. J. Phys. Chem. A, 86 (2012) 1294–1300.
[15] D.R. Tchuifon, S.G. Anaghoa, E. Njanja, J.N. Ghogomu, N.G. Ndifor-Angwafor, T. Kamgaing, Equilibrium and kinetic modelling of methyl orange adsorption from aqueous solution using rice husk and egussi peeling, Int. J. Chem. Sci., 12 (2014) 741–761.
[16] M. Kumar, R. Tamilarasan, Modeling of experimental data for the adsorption of methyl orange from aqueous solution using a low cost activated carbon prepared from *Prosopis juliflora*, Pol. J. Chem. Technol., 15 (2013) 29–39.
[17] A.A. Jalil, S. Triwahyono, S.H. Adam, N.D. Rahim, M.A.A. Aziz, N.H.H. Hairom, N.A.M. Razali, M.A.Z. Abidin, M. Mohamadiah, Adsorption of methyl orange from aqueous solution onto calcined Lapindo volcanic mud, J. Hazard. Mater., 181 (2010) 755–762.

[18] K.R. Ramakrishna, T. Viraraghavan, Dye removal using low cost adsorbents, Water Sci. Technol., 36 (1997) 189–196.
[19] S. Babel, T.A. Kurniawan, Low-cost adsorbents for heavy metals uptake from contaminated water: a review, J. Hazard. Mater., 97 (2003) 219–243.
[20] V.K. Garg, R. Kumar, R. Gupta, Removal of malachite green dye from aqueous solution by adsorption using agro-industry waste: a case study of *Prosopis cineraria*, Dyes Pigm., 62 (2004) 1–10.
[21] C. Namasivayam, S. Sumithra, Removal of direct red 12B and methylene blue from water by adsorption onto Fe(III)/Cr(III) hydroxide, an industrial solid waste, J. Environ. Manage., 74 (2005) 207–215.
[22] P. Janos, H. Buchtova, M. Ryznarova, Sorption of dyes from aqueous solutions onto fly ash, Water Res., 37 (2003) 4938–4944.
[23] V. Gupta, R. Kumarc, A. Nayaka, T. Saleh, M.A. Barakat, Adsorptive removal of dyes from aqueous solution onto carbon nanotubes: a review, Adv. Colloid Interface Sci., 193–194 (2013) 24–34.
[24] J.P. Wang, H.C. Yang, C.T. Hsieh, Adsorption of phenol and basic dye on carbon nanotubes/carbon fabric composites from aqueous solution, Sep. Sci. Technol., 46 (2010) 340–348.
[25] R. Coughlin, F. Ezra, Role of surface acidity in the adsorption of organic pollutants on the surface of carbon, Environ. Sci. Technol., 2 (1968) 291–297.
[26] K. Yang, B. Xing, Adsorption of organic compounds by carbon nanomaterials in aqueous phase: Polanyi theory and its application, Chem. Rev., 110 (2010) 5989–6008.
[27] G. McKay, M.S. Otterburn, A.J. Aga, Fuller's earth and fired clay as absorbents for dyestuffs external mass transport processes during adsorption, Water Air Soil Pollut., 24 (1985) 307–322.
[28] M.N. Sddiqui, Infrared study of hydrogen bond types in asphaltenes, Pet. Sci. Technol., 21 (2003) 1601–1615.
[29] M.F. Ali, M.N. Siddiqui, A.A. Al-Hajji, Structural studies on residual fuel oil asphaltenes by RICO method, Pet. Sci. Technol., 22 (2004) 631–645.
[30] M.N. Siddiqui, Catalytic pyrolysis of arab heavy residue and effects on the chemistry of asphaltene, J. Anal. Appl. Pyrolysis, 89 (2010) 278–285.
[31] Y. Akama, A. Tongb, M. Itoa, S. Tanakaa, The study of the partitioning mechanism of methyl orange in an aqueous two-phase system, Talanta, 48 (1999) 1133–1137.
[32] J.A. Dean, Lange's Handbook of Chemistry, 15th ed., McGraw-Hill, New York, USA, 1998.
[33] A. Cabeza, X. Ouyang, C.V.K. Sharma, M.A.G. Aranda, S. Bruque, A. Clearfield, Complexes formed between nitrilotris(methylenephosphonic acid) and M^{2+} transition metals: isostructural organic–inorganic hybrids, Inorg. Chem., 41 (2002) 2325–2333.
[34] M.R. Samarghandi, M. Hadi, S. Moayedi, F. Barjasteh Askari, Two-parameter isotherms of methyl orange sorption by pinecone derived activated carbon, Iran. J. Environ. Health Sci. Eng., 6 (2009) 285–294.
[35] G. Annadurai, R.S. Juang, D.J. Lee, Use of cellulose-based wastes for adsorption of dyes from aqueous solutions, J. Hazard. Mater., 92 (2002) 263–274.
[36] Z.M. Ni, S.J. Xia, L.G. Wang, F.F. Xing, G.X. Pan, Treatment of methyl orange by calcined layered double hydroxides in aqueous solution: adsorption property and kinetic studies, J. Colloid Interface Sci., 316 (2007) 284–291.
[37] J.H. Huang, K.L Huang, S.Q. Liu, A.T. Wang, C. Yan, Adsorption of Rhodamine B and methyl orange on a hypercrosslinked polymeric adsorbent in aqueous solution, Colloid. Surf., A, 330 (2008) 55–61.
[38] M. Kucukosmanoglu, O. Gezici, A. Ayar, The adsorption behaviors of methylene blue and methyl orange in a diaminoethane sporopollenin-mediated column system, Sep. Purif. Technol., 52 (2006) 280–287.
[39] Y. Iida, T. Kozuka, T. Tuziuti, K. Yasui, Sonochemically enhanced adsorption and degradation of methyl orange with activated aluminas, Ultrasonics, 42 (2004) 635–639.
[40] A. Mittal, A. Malviya, D. Kaur, J. Mittal, L. Kurup, Studies on the adsorption kinetics and isotherms for the removal and recovery of methyl orange from waste waters using waste materials, J. Hazard. Mater., 148 (2007) 229–240.
[41] M.J. Temkin, V. Pyzhev, Recent modifications to Langmuir isotherms, Acta Phys. Chim. Sin., 12 (1940) 217–222.
[42] R. Coşkun, C. Soykan, M. Saçak, Removal of some heavy metal ions from aqueous solution by adsorption using poly(ethylene terephthalate)-g-itaconic acid/acrylamide fiber, React. Funct. Polym., 66 (2006) 599–608.
[43] A. Ramesh, H. Hasegawa, T. Maki, K. Ueda, Adsorption of inorganic and organic arsenic from aqueous solutions by polymeric Al/Fe modified montmorillonite, Sep. Purif. Technol., 56 (2007) 90–100.